AUTOMATIC DRUSEN DETECTION FROM COLOUR RETINAL IMAGES

Saurabh Garg, Jayanthi Sivaswamy and Gopal Datt Joshi
Center for Visual Information Technology
IIIT Hyderabad, Hyderabad, India
saurabhgarg@students.iiit.ac.in, jsivaswamy@iiit.net, gopal@research.iiit.ac.in

ABSTRACT

The health of the retina deteriorates with age in some people due to the appearance of drusens. Drusens are accumulation of lipid and other waste material from different layers of the retina. These are markers of age-related macular degeneration (ARMD) as their increasing number generally indicates risk for ARMD, a leading cause of blindness in people above the age of 50. Morphological information of drusens is also crucial in determining the risk factor for ARMD. Colour retinal images are used presently to visually identify the presence of drusens. Automated detection and analysis can provide vital information about the quantity and quality of the drusens. In this paper, we report on two methods that we have developed to reliably detect and count drusens. The methods exploit the morphological characteristics of the drusens such as texture and their 3D profiles. We compare the results of using these two methods and make recommendations for automated drusen analysis.

KEY WORDS

Drusen detection, retinal image, ARMD, segmentation, medical image analysis

1 Introduction

Drusens are deposits of cellular waste that accumulate beneath the retina. They are the primary cause of age-related macular degeneration (ARMD), the leading cause of late-age blindness. The common method to screen for drusen is through retinal imaging. This paper focuses on methods to automatically detect and segment drusen in a retinal image without human supervision or interaction. These methods can be used to develop tools for screening, which help reduce costs by minimising the need for detailed scrutiny of large quantity of images by eyecare professionals. These methods could also be applied for treatment evaluation, by providing a quantified measurement of drusen presence that is *objective* and *repeatable*.

An accurate count of drusens in a colour retinal image, provides ample information about the extent of disease. Obtaining this information requires robust detection of drusen regions. The task of automatic detection poses various challenges. Drusens appear as yellowish, cloudy blobs in a retinal image. They exhibit no specific size or shape. The modification of size in individual drusens and their confluence seem to be an essential risk factor in developing macular degeneration. Drusens are classified as either hard or soft. Hard drusens tend to be smaller, more sharply defined and are generally less harmful than soft drusens. Soft drusens may be accompanied by other symptoms such as new vessel formation or fluid build-up in macula [1] [3]. The fuzzy boundaries of soft drusens pose a challenge in accurately locating the actual drusen region. A further challenge in segmenting drusens is the presence in the retina of other similar structures, such as optic disk, exudates and cotton wool spots. Some faint drusens can also appear similar to normal features of the retina, such as the background pattern caused by the choroidal vessels [3]. Furthermore, non-uniform illumination and variable contrast within the image (due to acquisition process of the image) make detection and segmentation task difficult. Thus the use of traditional segmentation methods are inadequate due to the nature of images as well as to the various aspects of drusen. These are some of the important factors which are needed to be addressed in order to perform an accurate detection and count of the drusens.

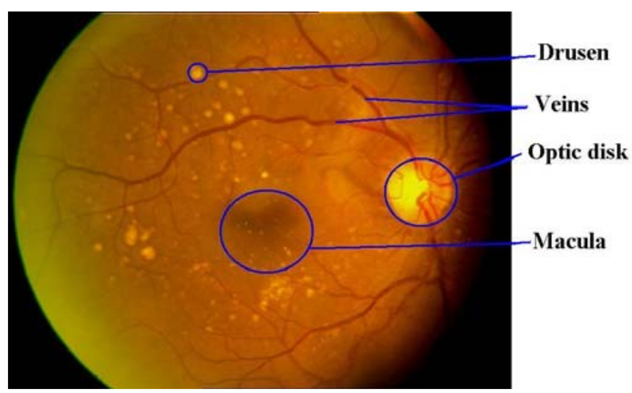

Figure 1. Sample colour retinal image.

There are very few attempts specifically on automated drusen detection or segmentation in retinal imagery. Sebh et al. [4] use a modified morphological operator to detect the brightest points (peaks) within individual drusens. Rapantzikos and Zervakis et al. [2] adopt an adaptive local histogram based method to identify an appropriate local threshold for segmenting each drusen. These methods however require a manual segmentation of the region of interest which is the region around the macula and between the 2 major veins (arcades). The manual segmentation eliminates the possibilities of false detection due to other interfering structures (for example, optic disk) and non-uniform illumination. The automatic segmentation of the region of interest itself is a challenging task. Thus, both the approaches do not provide complete solutions to the automatic detection task. Brandon et al. [3] report a technique to detect and segment drusen in full retinal images without human supervision or interaction. They use a multi-level approach, beginning with classification at pixel level and proceeding to the retinal, area, and then the image level. This is however computationally expensive and the results are dependent on a good set of training data.

The available approaches for the drusen detection task exploit very limited number of features of drusens. There are possibilities to use other drusen features in order to improve the detection. We have looked at drusen detection from two new perspectives. In the first one, we characterise a drusen by its texture which is distinct from that of the background. In the second one, we exploit the topographical profile of the drusens. The topographic perspective is derived from viewing the image as a surface wherein drusens appear as hilly regions. This perspective permits the drusen location to be in terms of a point on a hill or a plateau.

In this paper, we present the above new characterisations of drusens and assess their performance. The presentation in this paper is organised as follows. In the next section, we present the texture based approach and a multichannel filtering technique for segmentation. In section 3, we present a topographic model for drusens and present a curvature based detection method, followed by some concluding remarks.

2 Texture-based drusen detection

Texture segmentation and texture feature extraction are areas that have been well studied in the past. Statistical to structural or model based techniques have been used for texture based segmentation [5]. As seen from Figure 1, a drusen has a different texture pattern and colour in comparison with the background. A texture-based approach is hence an attractive alternative to the task of drusen segmentation. Furthermore, the texture of the drusen can be characterised in terms of the local energy. Local energy is defined as the sum of squared responses of orthogonal pairs of filters [6]. Gabor functions and more recently log-Gabor functions have been popular choices for such filters. In the next subsection, a local energy model using multi-channel log-Gabor filters is presented.

2.1 A local energy computation using multi-channel filtering

Local energy computation with Gabor filters is preferred since the filters can be easily tuned to different orientations and scale. For a given filter, its bandwidth decides the scale of the features that can be detected. The maximum bandwidth obtainable from a Gabor filter is only about 1 octave which is a disadvantage as it limits the feature size that can be captured. A log-Gabor filter on the other hand, allows large bandwidths, from 1 to 3 octaves, which makes the features more effective, reliable and informative.

Due to the singularity in the log-Gabor function at the origin, one cannot construct an analytic expression for the log-Gabor function in the spatial domain. Hence, the filter is designed in the frequency domain. On a linear scale, the transfer function of a log-Gabor filter is expressed as

$$\Phi_{(r_o,\theta_o)} = \exp\left\{-\frac{(\log(\frac{r}{r_o}))^2}{2(\log(\frac{\sigma_r}{r_o}))^2}\right\}\exp\left\{-\frac{(\theta-\theta_o)^2}{2\sigma_\theta^2}\right\} \tag{1}$$

where r_o is the central radial frequency, θ_o is the orientation, σ_θ and σ_r represent the angular and radial bandwidths of the filter, respectively.

The oriented local energy $E_{\theta_o}^{r_o}$ at every point (x,y) in the image defines an energy map. This is obtained as:

$$E_{\theta_o}^{r_o}(x,y) = (O_{\theta_o}^{r_o,even}(x,y))^2 + (O_{\theta_o}^{r_o,odd}(x,y))^2 \tag{2}$$

where $O_{\theta_o}^{r_o,even}(x,y)$, $O_{\theta_o}^{r_o,odd}(x,y)$ are the responses of the even and odd symmetric log-Gabor filters, respectively. Let $Z(r_o,\theta_o)$ be the filtered output. The responses of even and odd symmetric log-Gabor filters can be found as:

$$O_{\theta_o}^{r_o,even} = Re(Z(r_o,\theta_o)); \qquad O_{\theta_o}^{r_o,odd} = Im(Z(r_o,\theta_o)) \tag{3}$$

2.2 Experiment results

The green channel of the input image was used for all our experiments since the drusens were best represented in this channel. A filter bank with Log-Gabor filters at three different scales r_o and six different orientations θ_0: $0\,^\circ, 30\,^\circ, 60\,^\circ, 90\,^\circ$ and $150\,^\circ$ was used. The filter parameters were selected to span the frequency domain. Large radial bandwidth in the frequency domain implies small bandwidth in the spatial domain which helps in obtaining better localization of the segmented regions.

The filter parameters have been chosen to capture the high frequency components (edges) in the image such as in drusens. Since the high frequency content is also present in veins, for best results, they need to be suppressed. A simple technique was used to achieve this suppression. By noting that the veins appear as dark pixels in the green channel of the retinal image, all the dark pixels are replaced with the local mean of their neighborhood.

The algorithm was tested on different datasets. Figure 2 shows a sample image (only green channel) and the corresponding result. The results show that the energy is maximum at the locations of drusens. Thus, it is possible to easily segment the drusens using local energy. The

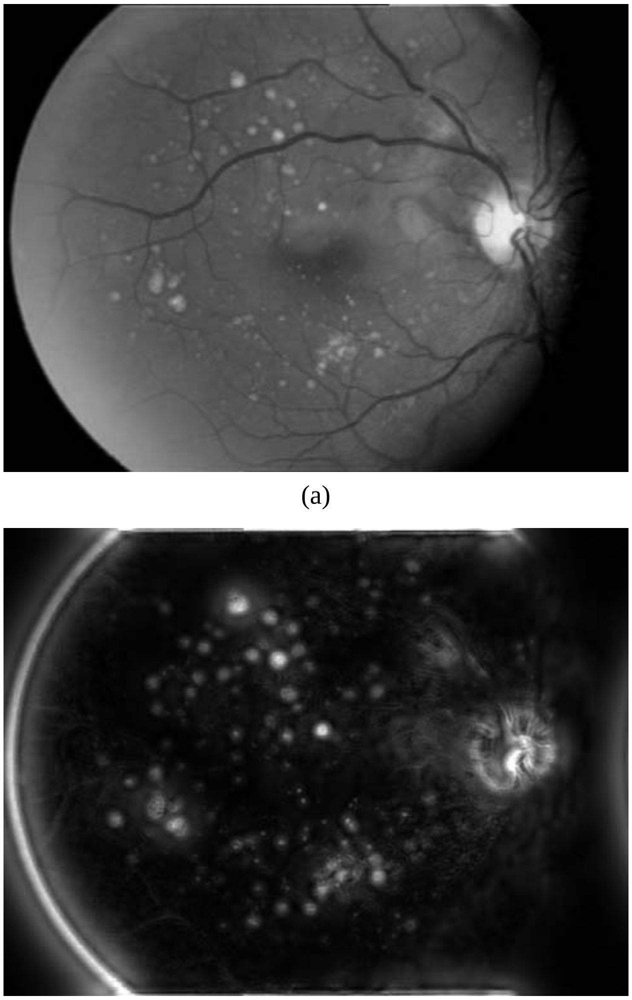

(a)

(b)

Figure 2. Results of multi-channel filtering. (a) Input image (Green channel), (b) Corresponding local energy output. Drusens appear as bright regions.

optic disk also is marked by high local energy and hence should be suppressed prior to the drusen detection. Our interest is to get an accurate count of the drusens and that will require further post processing of this result. A possible solution is to extract a closed boundaries for the drusens from the energy map and count each closed boundary as one drusen. However, the energy map indicates that obtaining a closed boundary will not be a simple task. To summarise, there appear to be two shortcomings with local energy based drusen detection: selection of tuning parameters that will work well across a wide range of images and obtaining a reliable drusen count. We look towards a model based approach to overcome these shortcomings.

3 Model-based drusen detection

Togographic models have been successfully used for feature detection in many applications [9] [10]. Visualising the 2D image function as a surface in 3D space leads to a different perspective of drusens as they have hilly profiles. In order to detect such a profile, a useful property, is the curvature of the image surface. Curvature has been successfully used to detect ridges, valleys, thin nets and crest lines from images. In general, curvature can be used to detect features where the image surface bends sharply. Such features are characterised by points of maximal curvature on the image surface.

The curvature at a point on the image surface is a measure of the bend in the surface along a particular direction. Because of this direction-specific nature of curvature, one can define the curvature of the image surface along a particular direction, in terms the curvature of the 1D profile of the image intensity values along that direction. Here, we present a measure of surface curvature of 2D digital images using an approach presented in [8] and review the definition for curvature of a 1D function.

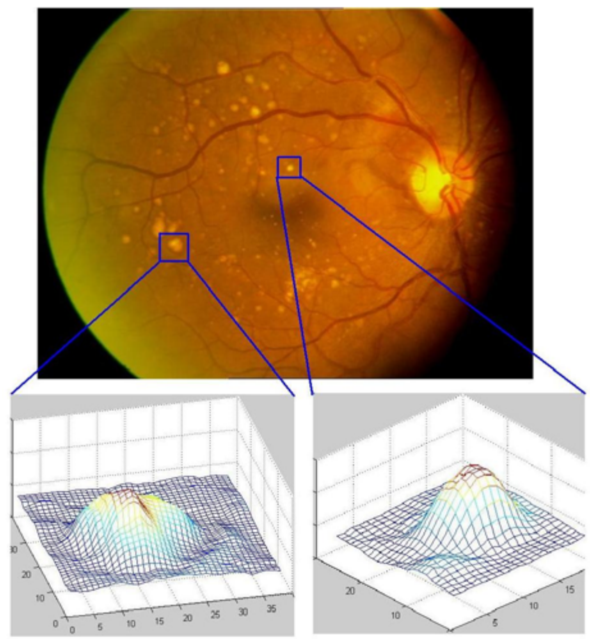

Figure 3. Sample retinal image and enlarged views of 3D profiles of some drusens.

Let $y = f(x)$ be a 1D function. Let the tangent at a point $P : x$ on this function make an angle θ with the x-axis as shown in Figure 4. If dl is the differential arc length at the point P, then the extrinsic curvature of the function $f(x)$ at this point is defined as:

$$k(x) = \frac{d\theta}{dl} = \frac{d\theta}{\sqrt{dx^2 + dy^2}} = \frac{\frac{d\theta}{dx}}{\sqrt{1 + (\frac{dy}{dx})^2}} \quad (4)$$

Since, θ is the angle made by the tangent with the x-axis, it can be computed as:

$$\theta = tan^{-1}\left(\frac{dy}{dx}\right) \quad (5)$$

Hence, the numerator term $\frac{d\theta}{dx}$ can be computed as:

$$\Upsilon(x) = \frac{d\theta}{dx} = \frac{d}{dx}\left[tan^{-1}\left(\frac{dy}{dx}\right)\right] = \frac{\frac{d^2y}{dx^2}}{1+\left(\frac{dy}{dx}\right)^2} \quad (6)$$

Substituting the above expression in equation 4, we get:

$$k(x) = \frac{\frac{d^2y}{dx^2}}{\left(1+\left(\frac{dy}{dx}\right)^2\right)^{\frac{3}{2}}} \quad (7)$$

which is the true curvature measure. As the point P moves on the curve $y = f(x)$, the tangent angle θ changes. This change over a given arc length dl is the true curvature measure $k(x)$. On a closer examination of equation 4, we can see that the numerator term $\Upsilon(x)$ represents the rate of change the tangent angle with respect to the projection of the arc length over the x axis. Comparing the equations 6 and 7, we see that the two expressions differ only by the power of the denominator. Significantly, $\Upsilon(x)$ will peak sharply at the locations of medial points of ridge profiles (as does $k(x)$), where the first derivative of the profile function vanishes and the second derivative is a negative maximum. Thus, $\Upsilon(x)$ is an alternative to the true curvature measure $k(x)$ since it also provides information about the rate of change of the tangent angle as a point moves along a curve [8]. In the case of 2D images, $\Upsilon(x)$ corresponds to a derivative of the angle made by a surface tangent line with the image plane, in some direction. Accordingly, we distinguish it from the true curvature measure, by calling it as the Surface Tangent Derivative (STD). We will use the STD as an estimate of the curvature of image surfaces.

Since drusens have a hilly profile, the STD can be used to detect them by detecting hill-like features in the images which are characterised by high values of STD in *all* directions. Here, we have used a hill detection algorithm presented in [8]. At every point in a given image, STD is computed in N different directions and maximum value of chosen among all N directions. A point is declared as a hill point if the value at that point is above a threshold value and maximum among its neighbours.

3.1 Experiment details

In our experiments STD computation was done in four different directions: $-45°, 0°, 45°, 90°$. We have used STD based hill detection to extract hill points in the image. The detected hill points can be due to a drusen at that location or due to noise. To remove the hill points occurring due to noise we retain those points whose value lies above a threshold. A low threshold value helps to pick even the faintest drusen but at the cost of some false negatives, while high threshold value will miss some of the faint drusens. Hence, the threshold value has to be carefully selected. In drusen detection, since the softer (faint) ones are more important, it is best to choose a low threshold. The false negatives can be suppressed later by using information about local context. The value of threshold was decided empirically and was kept fixed for all the images.

Figure 4. Results of multiscale hill point detection.

As drusens occur in various sizes and shapes, in order to detect all drusens it is best to perform a multiscale computation of STD. In our experiments, STD was computed at five different scales 3, 7, 11, 21 and 31 and the results were summed (logical OR). The result of hill detection on a sample image is shown in Figure 4. It can be seen that the hill points marked in green, coincide with drusen locations consistently well. Later, results were confirmed by the retina expert. It is quite possible that a large drusen will be characterised by more than one hill point using this approach which can adversely affect the count. This can be addressed by performing a local context-based culling of the hill points as a post processing step.

4 Discussion and conclusions

Drusens are markers of age-related macular degeneration (ARMD) as their increasing number generally indicates risk for ARMD. In this paper, we have investigated two new characterisations of drusens and developed methods to detect them from colour images. The existing drusen detection approaches can be broadly categorised into two classes of approaches. The first class of approaches directly extract the drusens from the image. Examples of such an approach are the texture- based detection presented in this paper and [2][3]. Whereas, approaches that belong to the second class first identify a seed point within the drusen region using either intensity maximas [4] or curvature maximas (presented here). The suitability of any drusen detection approach should be evaluated based on the actual aim of the work: to get an accurate count of drusens and to segment them for grading (identifying soft/hard drusens based on the area/size).

A drusen count in a given retinal image provides ample information about the potential risk for ARMD. The first class of approaches are not reliable in picking up small and faint drusens. Thus, they are not the best choice for the task in hand which is, getting a accurate count of drusens in the image. The second class of approaches are very reliable in picking up drusens of all sizes and types (bright or faint) in an image. Thus, the second class of approaches are recommended for obtaining an accurate count.

The task of grading drusens involves segmentation of entire drusen regions. The first class of approaches directly segment drusen regions and hence may appear to be best suited for grading. However, no assessment of the accuracy of the segmentation has been reported in the literature. Furthermore, a drawback of the methods in first class is the requirement of many pre-processing steps such as contrast stretching, etc., prior to the segmentation stage. These can potentially affect the reliability of the segmentation. By contrast, the hill-based drusen detection method we have presented does not require any preprocessing (except optic disk suppression) and hence will not affect the reliability of the results. Grading of drusens can be achieved using the second class of approaches as well by employing a robust region growing or region boundary finding (such as Snakes) techniques. In summary, since the second class of approaches have scope for providing an accurate count of drusens as well information for grading them they seem to be the most promising for automatic drusen detection.

References

[1] A. Abdelsalam, L. D. Priore and M. Zarbin, “Drusen in age related macular degeneration: Pathogenesis, natural course, and laser photocoagulation-induced regression,” Proc. Survey of Opthalmology 44 (1999).

[2] K. Rapantzikos, M. Zervakis, and K. Balas , “Detection and segmentation of drusen deposits on human retina: potential in the diagnosis of age-related macular degeneration,” Proc. International Conference on Image Processing 3 (2001) 1055–1058.

[3] L. Brandon and A. Hoover, “Drusen detection in a retinal image using multi-level analysis,” Proc. International Conference on Medical Image Computing and Computer-Assisted Intervention 2878 (2003) 618–625.

[4] Z. B. Sbeh and L. D. Cohen, “A new approach of geodesic reconstruction for drusen segmentation in eye fundus images,” IEEE Transaction on Medical Imaging 20(12) (2001) 1321–1333.

[5] T. Reed and J. Du Buf, “A review of recent texture segmentation and feature extraction techniques,” CVGIP: Image Understanding 57(3) (1993) 359–372.

[6] M.C. Morrone and R. Owens, “Feature detection from local energy,” Pattern Recognition Letters 1 (1987) 103–113.

[7] B.R Siva Chandra and J. Sivaswamy, “An analysis of curvature based ridge and valley detection,” Proc. International Conference on Acoustics Speech and Signal Processing (ICASSP), 2006.

[8] B. R. Siva Chandra, “Analysis of Retinal Angiogram Images,” M.S. thesis, IIIT Hyderabad, (2005).

[9] D. Eberly, R. Gardner, B. Morse, S. Pizer, and C. Scharlach, “Ridges for image analysis,” Journal of Mathematical Imaging and Vision 4 (1994) 353–373.

[10] O. Monga, N. Armande, and P. Montesinos, “Thin nets and Crest lines: Applications to Satellite Data and Medical Images,” Proc. IEEE Conference of Image Processing 2 (1995) 468–471.